

Field-Induced Three- and Two-Dimensional Freezing in a Quantum Spin Liquid

Y. Chen,¹ Z. Honda,² A. Zheludev,³ C. Broholm,^{1,4} K. Katsumata,² and S. M. Shapiro³

¹Department of Physics and Astronomy, Johns Hopkins University, Baltimore, Maryland 21218

²RIKEN (The Institute of Physical and Chemical Research), Wako, Saitama 351-0198, Japan

³Physics Department, Brookhaven National Laboratory, Upton, New York 11973-5000

⁴NIST Center for Neutron Research, National Institute of Standards and Technology, Gaithersburg, Maryland 20899

(Received 14 September 2000)

Field-induced commensurate transverse magnetic ordering is observed in the Haldane-gap compound $\text{Ni}(\text{C}_5\text{D}_{14}\text{N}_2)_2\text{N}_3(\text{PF}_6)$ by means of neutron diffraction. Depending on the direction of applied field, the high-field phase is shown to be either a three-dimensional ordered Néel state or a short-range ordered state with dominant two-dimensional spin correlations. The structure of the high-field phase is determined, and properties of the observed quantum phase transition are discussed.

DOI: 10.1103/PhysRevLett.86.1618

PACS numbers: 75.10.Jm, 75.30.Kz, 75.40.Cx

The one-dimensional (1D) integer-spin Heisenberg antiferromagnet (AF) demonstrates unique quantum-mechanical behavior that is inconsistent with the conventional semiclassical model of magnetism. Because of zero-point quantum spin fluctuations that destroy long-range order (LRO) even at $T = 0$, the ground state is a spin singlet with short-range (exponentially decaying) spatial spin correlations, and is often referred to as a “quantum spin liquid.” The main feature of the magnetic excitation spectrum is the so-called Haldane energy gap [1]. Quite remarkable is the behavior of 1D and quasi-1D integer-spin AFs in applied magnetic fields. The effect of the field is to suppress zero-point fluctuations, and restore a gapless spectrum. The result is a quantum phase transition at a certain critical field H_c , to a Néel-like state with long-range order that may be characterized as a “spin solid.” Thus, in an unusual twist, a *uniform* field induces *staggered* magnetization in quantum-disordered spin chains.

The magnetization process of a $S = 1$ 1D AF is now rather well understood theoretically [2–7]. For the isotropic case the problem was shown to be equivalent to Bose condensation in one dimension [3,8]. Many theoretical results were confirmed in experimental studies of real quasi-1D compounds. For a long time, however, the actual phase transition remained inaccessible for experimental investigation. In some materials (such as Y_2BaNiO_5 , for example [9]), the value of H_c is prohibitively high. In other compounds [e.g., $\text{Ni}(\text{C}_2\text{H}_8\text{N}_2)_2\text{NO}_2(\text{ClO}_4)$ [10]], the transition does not occur due to certain structural features, and is instead replaced by a broad crossover phenomenon [11–13]. A true phase transition at H_c has been experimentally observed only recently, in the quasi-1D $S = 1$ AF materials $\text{Ni}(\text{C}_5\text{D}_{14}\text{N}_2)_2\text{N}_3(\text{PF}_6)$ (NDMAP) [14–16] and $\text{Ni}(\text{C}_5\text{D}_{14}\text{N}_2)_2\text{N}_3(\text{ClO}_4)$ [17]. Specific heat, magnetization, and ESR studies have provided a comprehensive picture of the $H - T$ phase diagram [14–16], a refined version of which is shown in Fig. 1. Nevertheless, to date, the nature of the high-field phase remained undetermined, and no direct evidence of staggered LRO

has been obtained. In particular, preliminary neutron scattering experiments of Ref. [18] failed to detect any magnetic Bragg peaks above H_c . In the present Letter we report a high-field magnetic neutron diffraction study of NDMAP. We find that the high-field phase is characterized by a commensurate ordering of spin components perpendicular to the field direction. Surprisingly, the nature of the high-field phase is extremely sensitive to direction of applied field: depending on the experimental geometry, for $H > H_c$ the system develops either true 3D LRO or quasi-two-dimensional short-range order.

Magnetic properties of NDMAP are due to $S = 1$ Ni^{2+} spins that are assembled into AF chains running along the c axis of the orthorhombic $Pn\bar{m}n$ crystal structure ($a = 18.05$ Å, $b = 8.71$ Å, $c = 6.14$ Å). Haldane gap excitations and magnetic interactions in this system were previously investigated by means of zero-field inelastic

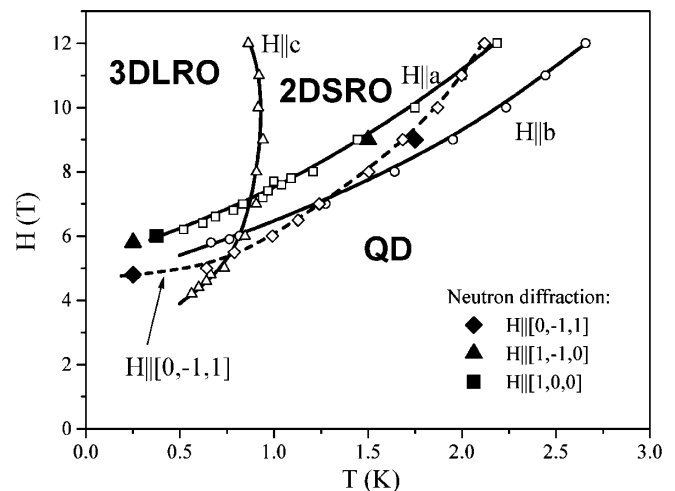


FIG. 1. Field-temperature phase diagram of NDMAP. A quantum-disordered (QD) phase with a gap is seen in low fields. The high-field phase is characterized by static long-range order (3D-LRO) or quasi-2D short-range order (2D-SRO). Open symbols from specific heat measurements, as in Ref. [15]. Solid symbols from neutron diffraction.

neutron scattering [19]. In-chain AF interactions are dominant and correspond to a Heisenberg exchange constant $J = 2.8$ meV. The triplet of Haldane excitations is split by easy- (a, b) plane anisotropy, and the gap energies are $\Delta_z = 1.9$ meV and $\Delta_\perp \approx 0.47$ meV, for excitations polarized along and perpendicular to the anisotropy axis, respectively. The coupling between chains along the b axis is rather weak, $J_y = 2 \times 10^{-3}$ meV, and barely detectable along a , $|J_x| < 5 \times 10^{-4}$ meV.

The present neutron diffraction experiments were performed at the SPINS cold-neutron three-axis spectrometer at the National Institute of Standards and Technology Center for Neutron Research. A 150 mg sample was mounted with the $(0, k, l)$, (h, h, l) , or (h, k, k) reciprocal-space planes in the scattering plane of the spectrometer. Most measurements were performed using $(^{58}\text{Ni guide}) - 80' - 80' - 240'$ or $(^{58}\text{Ni guide}) - 40' - 40' - 240'$ collimations, with a Be filter positioned in front of the sample to eliminate higher-order beam contamination, and $E_f = 5$ meV or $E_f = 3$ meV fixed final energy neutrons (typical energy resolution of 0.3 or 0.1 meV). Sample environment in all cases was a pumped He-3 cryogenic insert and a 9 or 7 T superconducting magnet, with the field applied vertically, i.e., perpendicular to the scattering plane.

True 3D commensurate AF LRO was observed in a crystal mounted in the (h, k, k) zone, with the magnetic field applied along the $[0, -1, 1]$ direction. At $T = 0.25$ K the transition occurs at $H_c = 4.8$ T, and manifests itself in the appearance of new Bragg reflections, at $(h, \frac{2n+1}{2}, \frac{2n+1}{2})$ (h —even integer; n —integer) reciprocal-space positions. No additional peaks were found at odd- h reciprocal-space points. Figures 2(a) and 2(b) show typical scans through the $(0, 0.5, 0.5)$ peak measured at $H = 9$ T applied field (symbols). The peaks are resolution limited along both the $(1, 0, 0)$ and $(0, 1, 1)$ directions. Wave vector resolution (Fig. 2, solid lines) was either calculated or directly measured in our experiment. The multiple peaks seen in the rocking scan in Fig. 2(a) result from sample mosaic. Geometrical limitations imposed by the use of the bulky 9 T magnet prevented us from measuring the width of the peak in the vertical $[0, 1, -1]$ direction. However, the substantial values of the b and c axis coupling constants, as well as the resolution-limited peak widths along a , where magnetic interactions are weakest, suggest that the observed reflections indeed have zero intrinsic width in all three directions, and represent true 3D long-range order. This is also consistent with the measured absolute values of magnetic intensities, as discussed below.

To determine the spin arrangement in the high-field ordered phase, intensities of $(0, 0.5, 0.5)$, $(2, 0.5, 0.5)$, $(4, 0.5, 0.5)$, $(2, 1.5, 1.5)$, and $(4, 1.5, 1.5)$ magnetic Bragg peaks in the (h, k, k) plane were measured in rocking scans at $T = 0.25$ K and $H = 9$ T. Magnetic intensities were brought to the absolute scale by comparing them to nuclear intensities measured in the same configuration at room temperature (the exact low-temperature structure

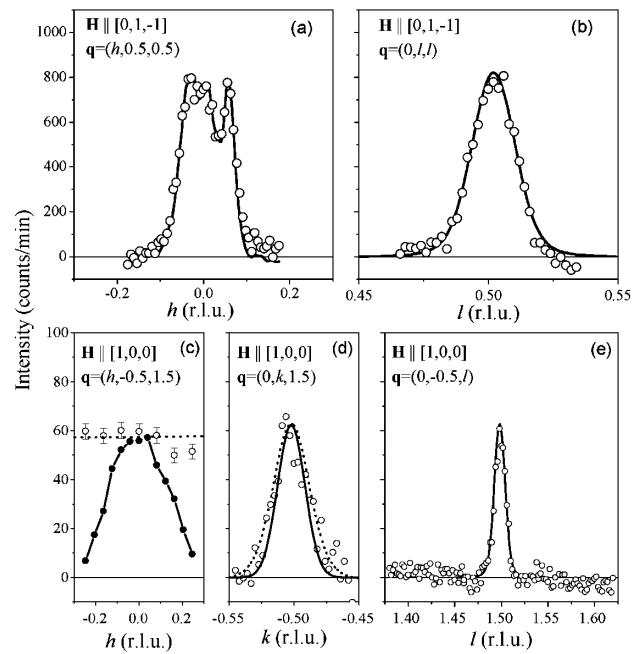


FIG. 2. Typical elastic scans (open symbols), showing magnetic Bragg scattering in NDMAP at $T = 0.25$ K, $H = 9$ T $\parallel [0, -1, 1]$ (a),(b) and $T = 0.375$ K, $H = 7$ T $\parallel [1, 0, 0]$ (c)–(e). The solid lines and symbols represent experimental wave vector resolution. Dashed lines as described in the text.

of NDMAP has not been determined to date). The data were analyzed using a simple collinear model. The strong (a, b) -easy plane anisotropy ensures that the ordered moment should be perpendicular to the chain axis. In-plane anisotropy is considerably smaller than the energy scale $g\mu_B H_c$ defined by the applied magnetic field [19], and the orientation of spins within the (a, b) plane is defined by the field direction. As the in-chain AF interactions are considerably larger than the Zeeman energy ($J \gg g\mu_B H_c$), the ordered moments align perpendicular \mathbf{H} . For a field applied along $[0, -1, 1]$ the spins are thus along $(1, 0, 0)$, as confirmed by recent ESR experiments [15]. This allows only one magnetic structure that would be consistent with the observed selection rule for magnetic Bragg peaks. Varying only the sublattice magnetization m , we obtained a good fit to the data ($\chi^2 = 1.6$) with $m = 1.13(5)\mu_B$. This value is to be compared to $m = 2\mu_B$ for a fully saturated $S = 1$ antiferromagnet.

The measured field dependence of the $(0, 0.5, 0.5)$ magnetic Bragg peak intensity at $T = 0.25$ K is shown in Fig. 3(a) (solid circles), and is consistent with our expectations for an easy-plane Haldane system at $T \rightarrow 0$. The data were analyzed assuming power-law field dependencies of the Bragg intensity and ordered moment: $I(H) \propto (H - H_c)^{2\beta}$. A fit of this equation to the data [Fig. 3(a), solid line] yields $H_c = 4.81(1)$ T and $\beta = 0.207(5)$. Since the transition at H_c occurs through a softening of the lowest-energy Haldane gap excitation [2], H_c is determined by the Haldane gap energies. It is straightforward

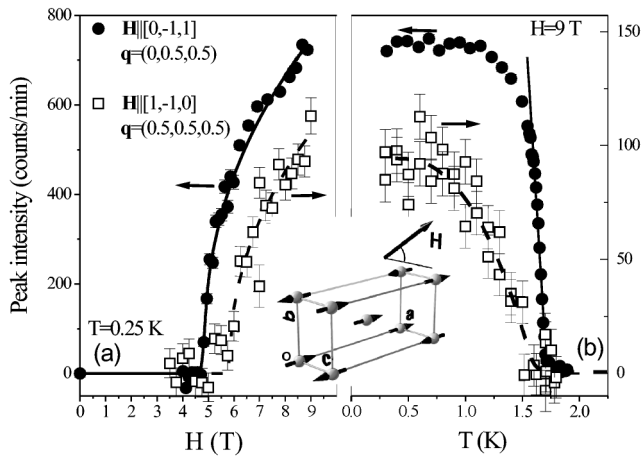


FIG. 3. Measured field (a) and temperature (b) dependence of the magnetic Bragg peak intensity in NDMAP for a field applied in the (b, c) plane. Solid lines are power-law fits to the data, as described in the text. Inset: A schematic view of the spin arrangement in the high-field phase, for the case $\mathbf{H} \parallel [0, -1, 1]$.

to show that for a magnetic field applied at angle α to the anisotropy axis c , the critical field is given by $\mu_B H_c = \Delta_z \Delta_{\perp} / \sqrt{g_z^2 \Delta_z^2 \cos^2 \alpha + g_{\perp}^2 \Delta_z \Delta_{\perp} \sin^2 \alpha}$. In this formula $g_z = 2.1$ and $g_{\perp} = 2.17$ are components of the Ni^{2+} gyromagnetic tensor along and perpendicular to the anisotropy axis, respectively [14]. For $\mathbf{H} \parallel [0, -1, 1]$, $\alpha = 54.8^\circ$ and this equation gives $H_c = 5.4$ T, in reasonable agreement with our experimental result. In the case of broken axial symmetry, for a *single* chain in a magnetic field at $T = 0$, the transition is expected to fall in the 2D Ising universality class, with magnetic field taking the role of effective temperature [3]. The order parameter critical exponent for this model is $\beta = 0.125$. For NDMAP, however, interchain interactions along the b axis can be considered substantial, and 3D Ising behavior, with $\beta \approx 0.31$, may be expected. The measured critical exponent falls in between these two values and is characteristic of a dimensional crossover regime.

The temperature dependence of the $(0, 0.5, 0.5)$ magnetic Bragg intensity measured at $H = 9$ T is shown in Fig. 3(b) (solid circles). An analysis of the data assuming a power law (solid line) yields $T_c = 1.7(1)$ K. The critical exponent was found to be indistinguishable from the mean field value $\beta = 0.5$, indicating that at $T \approx 1.5$ K the true critical region is too narrow to be investigated in the present experiment.

A striking result of this work is that for a magnetic field applied perpendicular to the chain axis, the high-field phase is no longer a 3D-ordered state, but has predominantly two-dimensional spin correlations. For the crystal mounted in the $(0, k, l)$ zone, at $T = 0.38$ K and $\mathbf{H} \parallel [1, 0, 0]$, magnetic scattering was detected at $(0, \frac{2n+1}{2}, \frac{2m+1}{2})$ (n, m -integer) reciprocal-space points above $H_c = 6$ T. k and l scans through the $(0, -0.5, 1.5)$ reflections contain well-defined peaks, as shown in Figs. 2(d) and 2(e) (symbols). Scans perpendicular to the (b, c) plane, however, re-

veal that the scattering is concentrated in Bragg rods along the $(1, 0, 0)$ direction, rather than Bragg peaks, as in the $\mathbf{H} \parallel [0, -1, 1]$ case. Figure 2(c) shows an h scan through the $(0, -0.5, 1.5)$ position that could be performed only in a limited range due to geometrical constraints. The measured intensity is independent of h . Note that the measured vertical resolution [Fig. 2(c), solid line] is sufficient to observe a well-defined Bragg peak. The rod nature of magnetic scattering implies that static spin correlations along the a axis are absent in the system, and that magnetic ordering occurs only within individual (b, c) planes. This is consistent with the a axis being the direction of weakest magnetic interactions. Similar behavior was observed for a magnetic field applied along the $[1, -1, 0]$ direction, where magnetic scattering was observed above $H_c = 5.8(2)$ T, at $T = 0.25$ K, and also found to be concentrated in Bragg rods parallel to the a axis. In this geometry, the rods cross the (h, h, l) scattering plane at $(\frac{2n+1}{2}, \frac{2n+1}{2}, \frac{2m+1}{2})$ (n, m -integer) positions. The measured field and temperature dependencies of magnetic diffraction intensity at $\mathbf{q} = (0.5, 0.5, 0.5)$ are shown in Fig. 3 (open symbols). A well-defined transition is observed in agreement with specific heat measurements (Fig. 1, diamonds).

The apparent Bragg rod intensity for $\mathbf{H} \parallel [1, 0, 0]$ and $\mathbf{H} \parallel [1, -1, 0]$ is substantially smaller than the intensity of magnetic Bragg peaks seen for $\mathbf{H} \parallel [0, 1, -1]$ (Fig. 2). This is due to the fact that in the 2D-ordered phase magnetic intensity is spread out through an entire Brillouin zone along the a axis, rather than being concentrated at $h = 0$. However, in the 2D phase, within each (b, c) plane, the actual ordered moment is similar to that in the 3D ordered state. The 2D ordered moment for $\mathbf{H} \parallel [1, 0, 0]$ and $\mathbf{H} \parallel [1, -1, 0]$ was deduced from an analysis of measured Bragg rod intensities, paying close attention to resolution effects associated with vertical angular acceptance of the spectrometer. A series of rocking scans across the rods were collected for $H = 7$ T $\parallel [1, 0, 0]$, $T = 0.38$ K, and $H = 9$ T $\parallel [1, -1, 0]$, $T = 0.25$ K, respectively. The data were normalized by the measured nuclear Bragg peak intensities. The two-dimensional spin structure was assumed to be collinear, with spins perpendicular to both the chain axis and \mathbf{H} in each case. Nearest-neighbor spins were assumed to be aligned antiparallel along both the b and c axes. This simple model was found to agree very well with the available data. The ordered moment was determined to be $m = 0.66(4)\mu_B$ and $m = 1.2(1)\mu_B$ for $H = 7$ T $\parallel [1, 0, 0]$, $T = 0.38$ K, and $H = 9$ T $\parallel [1, -1, 0]$, $T = 0.25$ K, respectively. The latter value agrees very well with the 3D ordered moment measured at $\mathbf{H} \parallel [0, -1, 1]$ at the same value of field and temperature.

A careful analysis of the scans across the Bragg rods for $\mathbf{H} \parallel [1, 0, 0]$ reveals a finite correlation length even within the quasi-2D ordered (b, c) planes. Along the direction of strongest coupling, i.e., along the chains, the magnetic peaks are resolution limited. This can be seen from Fig. 2(e), where the solid line represents experimental l

resolution. However, along the b axis, where magnetic interactions are weaker, the scattering rods are visibly broader than experimental resolution [Fig. 2(d), solid line]. Fitting the k scan to a Lorentzian profile convoluted with the resolution function [Fig. 2(d), dashed line] allows us to extract the intrinsic width of the rod that corresponds to a real-space correlation length $\xi_b = 100(20) \text{ \AA} \approx 10b$. The high-field phase in this case is thus characterized as a short-range ordered state with almost-perfect correlations along the chains and short-range correlations in the transverse direction.

This type of “spin freezing” in NDMAP is very similar to that recently found in the $S = 1/2$ quasi-1D AF SrCuO₂ [20]. For a two-dimensional Heisenberg system, the ground state is disordered and gapless for half-integer and odd-integer spin due to “instanton” topological defects [21]. If magnetic coupling along the third direction is sufficiently weak, as it is in NDMAP, it will not be able to restore LRO in the system due to pinning of such defects within each plane. The similar behavior of two very different systems, NDMAP and SrCuO₂, suggests that anisotropic spin freezing may be a rather general feature of quasi-low-dimensional antiferromagnets.

What makes the case of NDMAP special is that both true 3D LRO and 2D spin freezing can occur in the same sample, depending on the direction of applied field. Such behavior may result from the anisotropic nature of magnetic interactions along the a axis. Because of the very long a lattice spacing, these are expected to be largely dipolar in origin. The strength and even sign of such coupling depends on the orientation of the ordered moment, which, in turn, is defined by the direction of applied field. Changing the field orientation for NDMAP is thus a way to tune those magnetic interactions ultimately responsible for 3D LRO or spin-freezing behavior.

For the basic physics of Haldane spin chains, a very important experimental result is the observation of a *commensurate* ordering of *transverse* (relative to \mathbf{H}) spin components above H_c . Such staggered LRO in a quasi-1D material is a direct consequence of a divergence in the transverse spin correlation function for an isolated chain in an external field at $q = \pi$. Theory predicts that above H_c a divergence also exists in the longitudinal correlator, but at a field-dependent incommensurate wave vector [3,6]. No incommensurate magnetic peaks were found in our experiments on NDMAP. Of course, a divergent susceptibility in a single chain does not guarantee the appearance of LRO at the same wave vector in a 3D material. It is also conceivable that incommensurate elastic scattering in NDMAP appears at a different wave vector transfer perpendicular to the chain axis, due to anisotropy of interchain interactions, and thus escapes detection in the

present study. Further work will be required to fully resolve this issue.

In summary, our results provide direct experimental evidence of field-induced commensurate AF order in a Haldane-gap system, and are in good agreement with theoretical expectations. Specifics of interchain interactions in NDMAP result in a rich phase diagram with the high-field phase being either a true 3D ordered state or a highly anisotropic short-range ordered state.

The work at JHU was supported by the NSF through DMR-9801742. The work at Brookhaven National Laboratory was carried out under Contract No. DE-AC02-98CH10886, Division of Material Science, U.S. Department of Energy. This work used instrumentation supported by NIST and the NSF through DMR-9423101. The work at RIKEN was supported in part by a Grant-in-Aid for Scientific Research from the Japanese Ministry of Education, Science, Sports and Culture.

-
- [1] F.D.M. Haldane, Phys. Rev. Lett. **50**, 1153 (1983).
 - [2] I. Affleck, Phys. Rev. B **41**, 6697 (1990).
 - [3] I. Affleck, Phys. Rev. B **43**, 3215 (1991).
 - [4] T. Sakai and M. Takahashi, J. Phys. Soc. Jpn. **62**, 750 (1993).
 - [5] O. Golinelli, T. Jolicoeur, and R. Lacaze, J. Phys. Condens. Matter **5**, 1399 (1993).
 - [6] T. Sakai and H. Shiba, J. Phys. Soc. Jpn. **63**, 867 (1994).
 - [7] P.P. Mitra and B.I. Halperin, Phys. Rev. Lett. **72**, 912 (1994).
 - [8] V.N. Nicopoulos and A.M. Tsvelik, Phys. Rev. B **44**, 9385 (1991).
 - [9] See reference lists in G. Xu *et al.*, Phys. Rev. B **54**, R6827 (1996).
 - [10] See reference list in L.P. Regnault, I. Zaliznyak, J.P. Renard, and C. Vettier, Phys. Rev. B **50**, 9174 (1994).
 - [11] M. Chiba *et al.*, Phys. Rev. B **44**, 2838 (1991).
 - [12] T. Kobayashi *et al.*, J. Phys. Soc. Jpn. **63**, 1961 (1992).
 - [13] M. Enderle, L.-P. Regnault, C. Broholm, D.H. Reich, I. Zaliznyak, M. Sieling, and B. L. üthi (unpublished).
 - [14] Z. Honda, H. Asakawa, and K. Katsumata, Phys. Rev. Lett. **81**, 2566 (1998).
 - [15] Z. Honda, K. Katsumata, M. Hagiwara, and M. Tokunaga, Phys. Rev. B **60**, 9272 (1999).
 - [16] Z. Honda, K. Katsumata, Y. Nishiyama, and I. Harada, cond-mat/0006295, 2000.
 - [17] Z. Honda *et al.*, J. Phys. Condens. Matter **9**, L83 (1997).
 - [18] Y. Koike, N. Metoki, Y. Mori, T. Kobayashi, T. Ishii, and M. Yamashita, J. Phys. Soc. Jpn. (to be published).
 - [19] A. Zheludev, Y. Chen, C. Broholm, Z. Honda, and K. Katsumata, cond-mat/0003223 [Phys. Rev. B (to be published)].
 - [20] I.A. Zaliznyak *et al.*, Phys. Rev. Lett. **83**, 5370 (1999).
 - [21] F.D.M. Haldane, Phys. Rev. Lett. **61**, 1029 (1988).